Visualization and Modal Analysis of Guided Waves from a Defect in a Pipe

Muhammad NOR SALIM, Takahiro HAYASHI, Morimasa MURASE, and Shoji KAMIYA
Department of Mechanical Engineering, Nagoya Institute of Technology, Nagoya, 466-8555, Japan

Many of the commercial guided wave pipe inspections are using axisymmetric torsional mode T(0,1) as well as a longitudinally vibrating L(0,2) mode as incident wave in guided wave pipe inspections since the torsional mode has prominent characteristics of low attenuation and non-dispersion. However, reflected waves from defects in a pipe contain many modes other than the incident torsional mode, and the complex reflected wave propagation sometimes prevent us to find the defects. Therefore, in this study, visualization of guided wave propagations around the full circumference of a pipe is carried out. A Laser Doppler Vibrometer (LDV) and a 6-axis robot arm are used for scanning over the curved surfaces. The visualizations of guided wave propagations from defects are shown in the in-plane and out-of-plane vibrations to analyze mode conversions at defects in more detail.

Keywords: Visualization, Mode conversion, Curved surfaces scanning, Guided wave, Laser Doppler Vibrometer

1. Introduction

Guided wave pipe inspections provide a long-range pipe inspection from a single measurement point. This new approch in pipe inspection has been studied in detail by many researchers such as Rose et al.[1-4] and Cawley et al.[5-8] that proposed a number of inspection techniques using torsional modes of guided wave as well as flexural modes and focusing technique. These guided wave pipe inspections are differerent from traditional point-by-point bulk wave methods. Guided wave inspection, however, has special difficulties compared to the conventional point-by-point bulk wave methods, because of guided wave propagations occur in many modes with different wave structures and velocities.

In order to avoid the complexities in detected waveforms, most of the developed equipments for guided wave pipe inspection use the axisymmeteric torsional mode T(0,1) to find the specific defects in oil, gas and chemical pipelines for petrochemical industries.[9,10] Using an axisymmetric mode transducer, this axisymmetric guided wave will vibrate the pipe wall in the circumferential direction, and then, defect in pipe at inaccessible areas can be identified easily from the reflected waves shown in the measured RF signal. Nevertheless, the amplitude of the reflected waves are associated with the features of defect and sometimes appears in very small signals which difficult to be measured.[11-14] This is an example due to the mode conversion during the guided wave pipe inspection where the waves are reflected in different modes from the incident wave.

The behaviors of guided wave propagation in pipe from a circumferential and an oblique defects are presented in this paper to explain the mode conversions occur around these defects in pipes. These guided wave propagations are revealed using an imaging technique that use a large number of RF signals measured on the curved surfaces of pipes by a non-contact measurement technique using a Laser Doppler Vibrometer (LDV) and a robot arm that scans over the full circumference around defects in pipes. The guided wave propagation in pipes were visualized in in-plane and out-of-plane vibrations to analyze the mode conversions occur around defects when the pipes were introduced with an axisymmeteric mode T(0,1) from a magnetostrictive sensor.

2. Measurement Method

2.1 *Measurement system*

Figure 1 shows the entire laser scanning system that excites axisymmetric mode T(0,1) at central frequency of 70 kHz from a magnetostrictive sensor attached around the

pipe and measured the guided wave around defect in the pipe using a LDV.[15,16] This measurement were made for two test pipes with different artificial defects in aluminum pipes with dimension of 4 m in length, 110 mm in outer diameter and 3.5 mm in thickness. The artificial defects were made on the pipe surfaces stretching in the circumferential direction as Fig. 2(a) and in the oblique direction at angle of about 45° to the horizontal direction as Fig. 2(b). Both defects were scratched by a round file in size of about 40 mm in length, 10 mm in width and 2 mm in depth at 500 mm from a pipe end.

Scanning over a curved surface on pipe is different from scanning on flat surface of a plate, which the RF signals can be measured by moving the focal point of the LDV using a 3-axis linear guide system. On curved surface scanning, the focal point and direction of the incident beam have to be controlled to retain the sensitivity of the LDV during the measurement. This measurement was performed by a 6-axis robot arm that holds the LDV and moves its posture to aim the focal point of the LDV at the determined direction of the incident beam on any locations in the scanning region.[15,17] The magnetostrictive sensor, scanning regions and defect are located as shown in Fig. 3(a). Guided wave propagations around full circumference of the pipes are measured in the scanning regions depicted in Fig. 3(b), which the RF signals were measured at many points on the surface of retro-reflection tapes attached on the regions with sufficiently small distance compared to wavelength of the guided waves. As these retro-reflection tapes covered with small beads reflect the laser beam in the incident direction, both in-plane and out-of-plane vibrations can be measured. RF signals are collected separately from 6 regions in full circumference of the pipe around Row I and Row II and then the 12 images are merged into a large image in the visualization of guided wave propagation as shown in Fig. 3(c).[17]

2.2 Visualization of in-plane and out-of-plane mode vibrations

An axisymmetric torsional mode T(0,1) was applied by the magnetostrictive sensor as an incident wave and collect the waveforms around the artificial defect with LDV. Even though the incident wave T(0,1) is an axisymmetric mode with in-plane vibration, the reflected waves from a defect consists of non-axisymmetric modes with out-of-plane mode vibration as well as in-plane mode vibration. The LDV equipped with a robot arm can measure these RF signals that contain the components of in-plane and out-of-plane vibrations of torsional, longitudinal and flexural modes. [9,10]

The measurements of vibrations in a pipe is detailed in Fig. 4 where RF signals are measured in two different laser beam directions of θ to the pipe surface as S_1 and S_2. These

signals are measured at each scanning position from two different directions of laser beam to visualize the in-plane and out-of-plane mode vibrations reflected from a defect. In-plane vibration velocity V_{in} and out-of-plane vibration velocity V_{out} at the current measurement position on the pipe are obtained from the signals S_1 and S_2, as represented in the following expressions:

$$V_{in} = \frac{S_1 - S_2}{2 \cdot \cos\theta} \tag{1}$$

$$V_{out} = \frac{S_1 + S_2}{2 \cdot \sin\theta} \tag{2}$$

RF signals of in-plane and out-of-plane vibrations for each scanning region were obtained from the collected RF signals measured at the incident angle θ of 45˚ from the pipe surface as illustrated in Fig. 4. A large number of in-plane and out-of-plane vibrations obtained from the eqs. (1) and (2) were used to emphasize the reflected waves of the RF signals that reflected in very small signals compared to the amplitude of incident wave. The signal processing is necessary prior to visualization of the guided wave propagation in pipe for both in-plane and out-of-plane mode vibrations. This is due to interference between the reflected wave and incident wave around defect that degrade the reflected waves of RF signals. The inspection in pipe with circumferential defect were performed using a signal processing that used a number of waveforms of RF waves, which measured at different locations closed to the current location in longitudinal direction. These waveforms were shifted to match the phase of the reflected wave at the current location and averaged to emphasize the reflected wave at the current location. This signal processing is successfully emphasized the reflected waves from the circumferential defect in pipe for both in-plane and out-of-plane mode vibrations.[17,18] However, the reflected waves from oblique defect are reflected mainly in non-axisymmetric mode than the axisymmetric mode. Therefore, we applied another signal processing that shifted a number of waveforms closed to the current location to match the phase of the incident waves at the current location and remove the incident wave from the RF signals.[19]

3. Results and Discussion

Guided wave propagations in a pipe with a circumferential defect are visualized in both in-plane vibration, Fig. 5 and out-of-plane vibration, Fig. 6. Visualizations of guided

wave propagations exhibit reflected waves when the incident wave hits on the circumferential and oblique defects in the pipes. Right regions of Fig. 5(a) indicated that most of ultrasonic energy from the incident T(0,1) mode reflects in the same mode as the incident wave and travels at the maximum speed about 3000 m/s towards the magnetostrictive sensor. [15] A number of guided wave modes are strongly initiated from the circumferential defect after t=300 μs until approaching t=390 μs. These reflected waves propagate parallel to the axial direction of the pipe as depicted in Figs. 5(a), 5(b) and 5(c). On the other hand, Fig. 6(a) shows the out-of-plane vibration with reflected waves observed in the left regions at t=362 μs. Considering the distance between the magnetostrictive sensor and the defect and the travelling time, these reflected waves were caused by the faster waves than the T(0,1) incidence, and the faster waves should be longitudinally vibrating modes with higher group velocities excited by the magnetostrictive sensor as well as the T(0,1) mode. Interestingly, the result of the out-of-plane vibration Fig.6(a) exhibits that mode conversions occurred at the edges of the circumferential defect shown in the right regions of Figs. 6(a) and 6(b). These are higher order of torsional and flexural guided wave propagations, which reflected inclined to the centerline of defect and travel at the speed lower than the reflected wave explained in Fig. 5.[9-14] The incident T(0,1) mode is also reflected as shear vertical wave that vibrates perpendicular to the surface of a pipe shown in the right regions of Fig. 6(c), which travels at the speed lower than the waves explained in Figs. 6(a) and 6(b).

Figures 7 and 8 show the visualization of guided wave propagations in a pipe with oblique defect. Since both circumferential and oblique defects are made at the same distance from the magnetostrictive sensor, reflected waves appeared at the same time in the both pipes.. The reflected waves from the oblique defect are also observed between t=300 μs and t=390 μs in both in-plane and out-of-plane vibrations. These results exhibit that the reflected waves of T(0,1) mode are reflected in oblique direction according to inclined angle of the defect and propagate spirally towards the magnetostrictive sensor. These spiral propagations of the reflected waves are observed in both visualizations of guided wave propagations in the in-plane and out-of-plane vibrations. The spirally propagating wave can be considered as the superposition of multiple modes of higher order torsional and flexural modes with low group velocities. [9-14]

The results for the oblique defect significantly show that the reflected waves of T(0,1) mode in the out-of-plane vibration has larger amplitude than one of the in-plane vibration as shown in Figs. 7 and 8. This indicated that mode conversions occur more largely in the pipe with oblique defect, in which the incident wave T(0,1) mode with the in-plane

vibration were converted into out-of-plane vibrations as shown in Fig. 8.

Different shapes of reflected waves were also observed in the visualization of in-plane and out-of-plane vibrations from the oblique defect. The reflected waves occur in the in-plane vibration shown in Fig. 7 propagated in wider area than reflected waves in the out-of-plane vibration shown in Fig. 8. This is due to the interference of the reflected waves initiated from both edges of the oblique defect that occur in the in-plane mode vibration. On the other hand, reflected waves in the out-of-plane vibration are concentrated at centerline of the spiral path. This is due to the out-of-plane component of reflected waves occurred along center of the surface of oblique defect which reflected perpendicular to centerline of the oblique defect.

These visualizations of the guided wave propagations in the full circumference of pipe from circumferential and oblique defects represent the axially symmetric features and non-axially symmetric features in a pipe respectively. The experimental results exhibit that the mode conversions occur at a circumferential defect in a pipe are insignificant compared to an oblique defect in a pipe. This propagation of incident wave T(0,1) mode to the circumferential defect in pipe is similar to propagation of shear horizontal (SH) incident wave into a solid media likes plates. Reflected waves of the T(0,1) mode from a defect are generated in the in-plane vibration which are not affected by containing liquid in a pipe and insulation tapes on a pipe. These low attenuation signals result high detectability of the reflected waves from axially symmetric defects in pipes that extends the range of guided wave pipe inspection.[8,9,11-13] The results also indicate that the circumferential defect in the pipe can be identified using an axisymmetric mode transducer which measures the reflected waves of T(0,1) mode in pipe. On contrary, the pipe with oblique defect exhibits a significant mode-conversions of the incidence T(0,1) mode. Most of the incident wave of T(0,1) mode are converted into out-of-plane reflected waves which propagate spirally in the pipe towards the magnetostrictive sensor. These out-of-plane reflected waves have large effect in attenuation from containing liquid in a pipe and insulation tapes on pipe surface. These high attenuated signals result in low SN ratio in the reflected waves from the oblique defect in pipe that limits the range of guided wave pipe inspection. The results also indicate that the oblique defect in pipe can be identified using a non-axisymmetric mode transducer if placed facing the spirally reflected wave in pipe.

4. Conclusions

In-plane and out-of-plane guided wave propagations are successfully visualized around the full circumference of pipes with circumferential and oblique defects. Visualization

of the guided wave propagations around defects in pipes reveal the behavior of reflected waves occurred from the axially and non-axially symmetric defects in pipes as shown the pipe with a circumferential defect and an oblique defect respective. The profiles of the guided wave propagations are shown clearly in the visualization results for the reflected waves from circumferential filling defect that reflected in longitudinal direction and similarly to the reflected waves from oblique filling defect that reflected spirally in pipe. The information of the reflected waves is important in order to develop new sensors and inspection technique for specific defects in pipes.

Acknowledgements

This research was partially supported by the Industrial Technology Research Grant Program in 2007 from the New Energy and Industrial Technology Development Organization (NEDO) of Japan and Encouragement of Young Scientists (A) program in 2007 from Grants-in-Aid for scientific research.

1) J.L. Rose : *Ultrasonic Waves in Solid Media* (Cambridge University Press, U.K., 1999) pp.154-162.

2) T. Hayashi, K. Kawashima, Zongqi Sun and J.L. Rose : J. Pressure Vessel Technology **127** (2005) 317.

3) Zongqi Sun, Li Zhang, and J.L. Rose : J. Pressure Vessel Technology **127** (2005) 471.

4) Jian Li and J.L. Rose : Ultrasonics **44** (2006) 35.

5) M.J.S. Lowe, D.N. Alleyne, and P. Cawley : Ultrasonics **36** (1998) 147.

6) R. Long, M.J.S Lowe, and P. Cawley : Ultrasonics **41** (2003) 509.

7) D.N. Alleyne, and P. Cawley : Review of Progress in Quantitative NDE **14** (1995) 2073.

8) C. Aristegui, M.J.S. Lowe and P. Cawley : Ultrasonics **39** (2001) 367.

9) T. Hayashi : Jpn. J. Appl. Phys. **47** (2008) 3865.

10) T. Hayashi, K. Kawashima, and J.L. Rose : Engineering Materials **270-273** (2004), 410.

11) D.N. Alleyne, M.J.S. Lowe, and P. Cawley : J. Appl. Mech. **65** (1998) 635.

12) M.J.S. Lowe, D.N. Alleyne, and P. Cawley : J. Appl. Mech. **65** (1998) 651.

13) A. Demma, P. Cawley and M.J.S Lowe : J. Acoust. Soc. Am. **114** (2) (2003) 611.

14) Z.L. Li, J.D. Achenbach, I. Komsky, and Y. C. Lee : J. Appl. Mech. **59** (1992) 349.

15) T. Hayashi, Y. Kojika, K. Kataoka and M. Takikawa, Review of Progress in Quantitative NDE **27A** (2007) 178.

16 H. Kwun, S. Y. Kim and G. M. Light : Materials Evaluation **61-1** (2003) 80.

17) Nor Salim Bin Muhammad, M. Murase, T. Hayashi, and S.Kamiya : Review of progress in Quantitative NDE, (submitted Oct 2008).

18) S. Yashiro, J. Takatsubo, H. Miyauchi and N. Toyama : NDT & E International **41** (2) (2008) 137.

19) J. Takatsubo, B. Wang, H. Miyauchi, K. Urabe, H. Tsuda and N. Toyama : Proc. (Spring Conf., 2008); Japan Society for Non-Destructive Inspection, 21 [In Japannese].

Fig. 1 Scanning system of guided wave propagation on pipe surface.

Fig. 2 Artificial defects made on pipe surfaces.

Fig. 3 Test pipe and visualization regions.

Fig. 4 Measurement of both in-plane and out-of-plane vibrations at angle θ of incident beam.

Fig. 5 In-plane mode vibration of circumferential defect in pipe.

Fig. 6 Out-of-plane vibration of circumferential defect in pipe.

Fig. 7 In-plane mode vibration of oblique defect in pipe.

Fig. 8 Out-of-plane vibration of oblique defect in pipe.

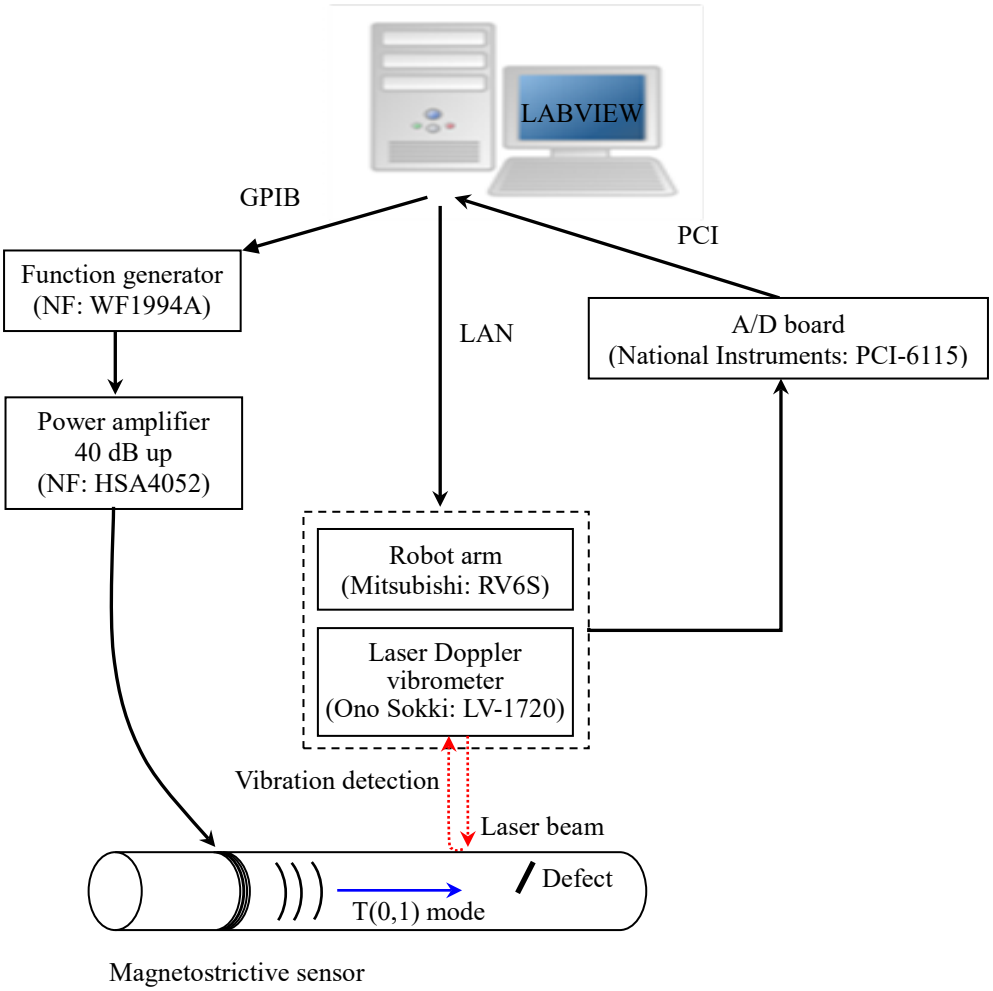
LABVIEW
GPIB
PCI
LAN
Function generator
(NF: WF1994A)
Power amplifier
40 dB up
(NF: HSA4052)
A/D board
(National Instruments: PCI-6115)
Robot arm
(Mitsubishi: RV6S)
Laser Doppler
vibrometer
(Ono Sokki: LV-1720)
Vibration detection
Laser beam
Defect
T(0,1) mode
Magnetostrictive sensor

Fig. 1

(a) Circumferential defect

(b) Oblique defect

Fig. 2

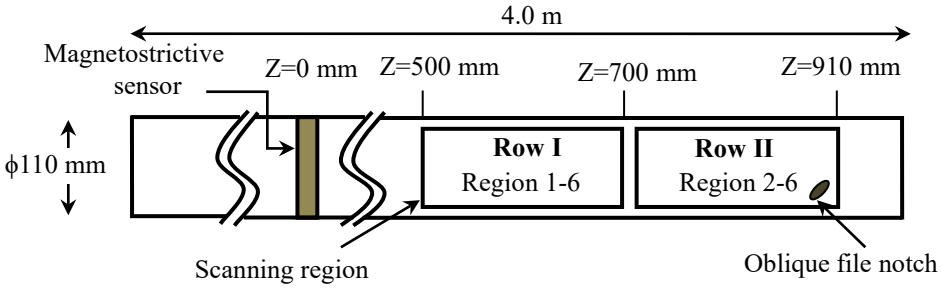

a) Configuration of test pipe

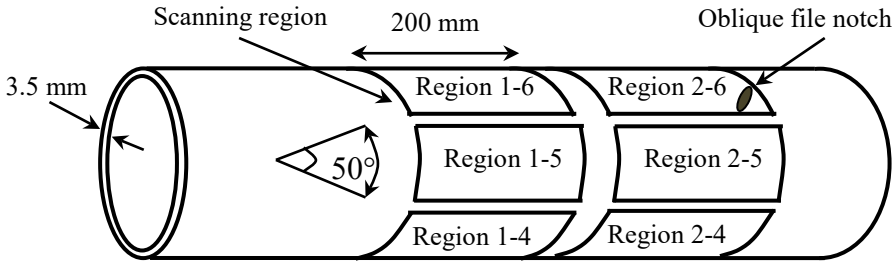

b) Scanning regions on pipe surface

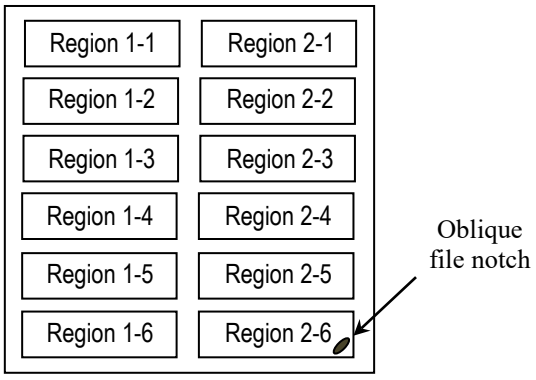

c) Visualized inspected areas on pipe surface

Fig. 3

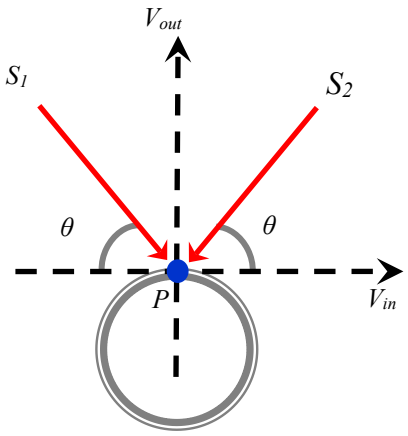

Cross section of pipe

where,

S_1 : first measurement of RF signal

S_2 : second measurement of RF signal

P : current scanning position on pipe surface

V_{in} : in-plane mode vibrations

V_{out} : out-of-plane mode vibrations

θ : angle of incident laser beam

Fig. 4

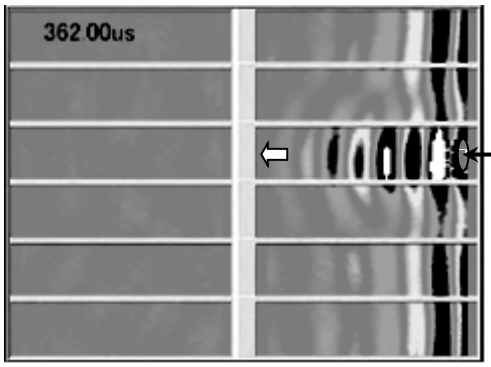

(a) t=363 μs

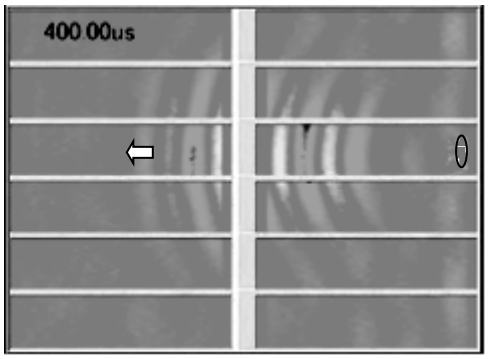

(b) t=400 μs

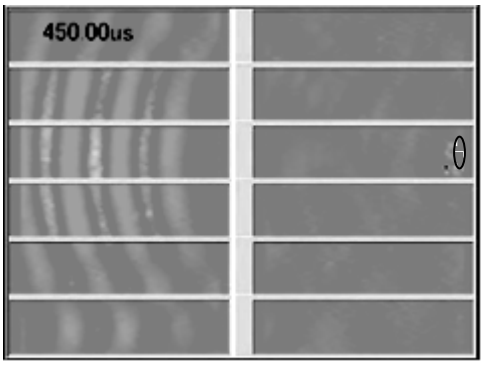

(c) t=450 μs

Fig. 5

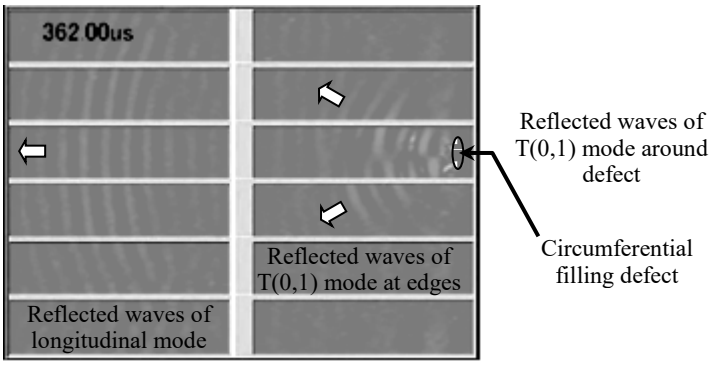

(a) t=362 μs

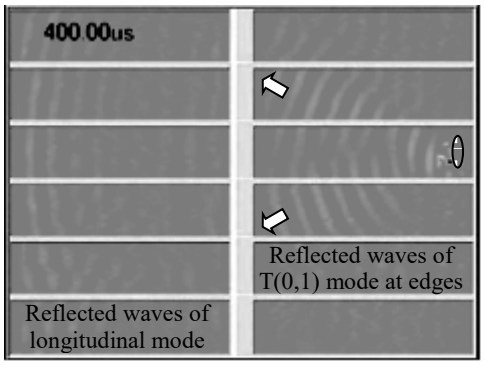

(b) t=400 μs

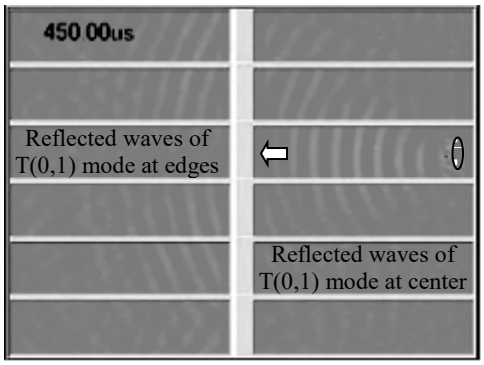

(c) t=450 μs

Fig. 6

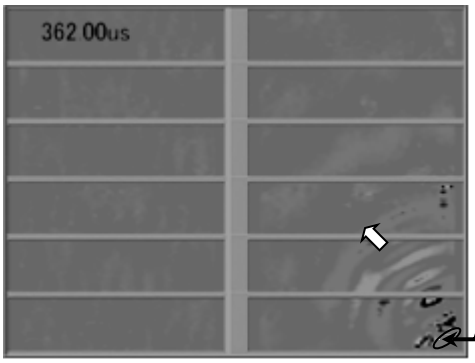

(a) t= 362 μs

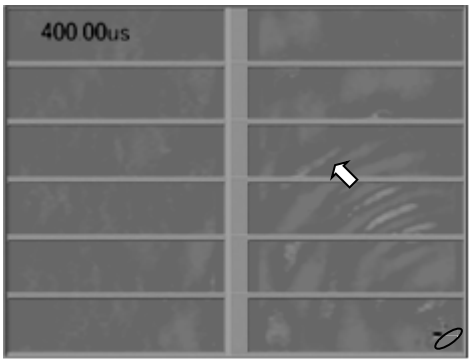

(b) t= 400 μs

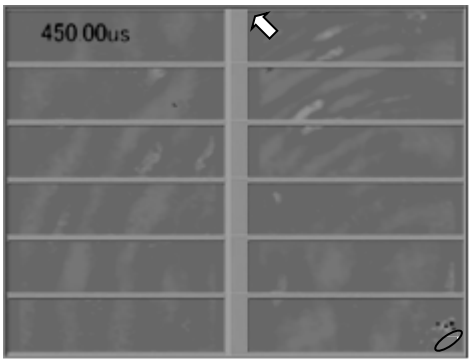

(c) t= 450 μs

Fig. 7

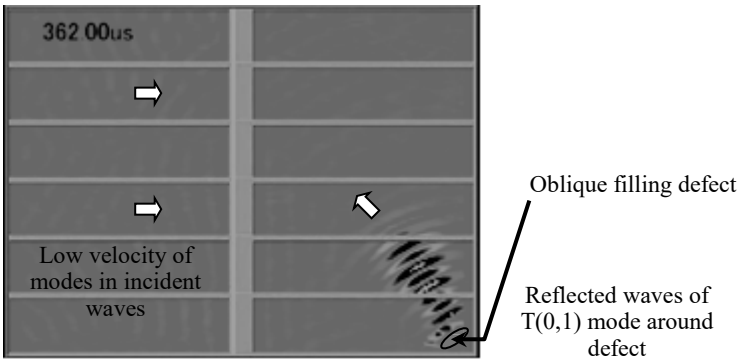

(a) t=362 μs

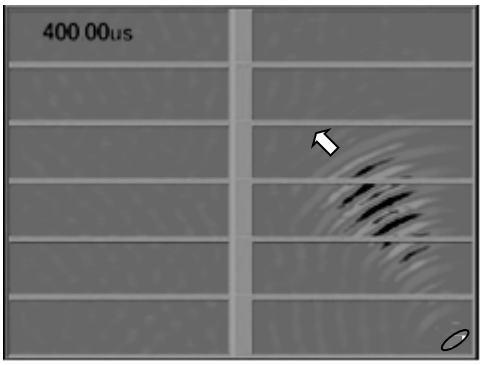

(b) t=400 μs

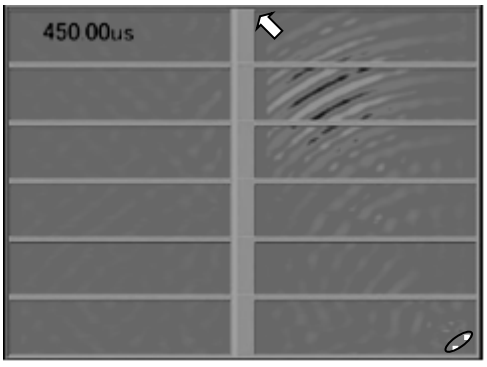

(c) t=450 μs

Fig. 8